Melting of Ice Spheres in Nearly Isotropic Turbulence With Zero Mean

Herricos Stapountzis[1,*], Theodoros-Gaitanis Dimitriadis[1], Konstandinos Giourgas[1], Konstandinos Kotsanidis[1]

[1]Department of Mechanical Engineering, University of Thessaly, Volos, Greece
*corresponding author: erikos@uth.gr

Abstract The melting of ice spheres of diameter 0.0375 m has been observed by flow visualization in a water tank and in an air turbulence chamber. In both facilities the generated turbulence was nearly isotropic and homogeneous with zero mean velocity. For the water experiments two oscillating grids were used and for the air experiments synthetic air jets. The latter type of flow was also heated in order to examine the added effect of temperature fluctuations on melting. The quantity of main concern was the change in the linear dimensions of the sphere during melting in order to relate it to the effect of turbulence intensity and also compare the impact of turbulence on the melting in still fluid medium. It was found that turbulence greatly reduces melting times and in combination with buoyancy forces can lead to elongated shapes. The melting of a pair of spheres was also examined.
Keywords: Melting, Ice Sphere, Heat Transfer, Isotropic Turbulence, Stefan Problem, Hailstone

1 Introduction

Melting of solid objects is found in many situations of industrial and environmental nature such as melting of ice in heat exchangers, solid dissolution in liquids, melting of silicon crystals for microelectronic applications, deep penetration welding, metal casting technology, melting under various gravity levels in space, thawing of frozen foods, but also in melting of hail in meteorology and icebergs in glaciology and oceanography, crystal growth, magmatic crystallization etc. Due to the influence of change in phase, the characteristics of momentum, heat and species transport between the phases are markedly different from those between two phases without phase change, especially if transport is enhanced by forced convection and also the presence of turbulence. A moving boundary develops between the phases, which has to be determined in space and time. Thermal energy is liberated on this boundary in the form of latent heat. Since the mixing of the melt with the supply fluid flow is not in thermal equilibrium and the latent heat is not only removed by conduction, the mathematical conditions on the boundary are non-linear, making the solution of the so called "Stefan moving boundary problems" very difficult, even in one dimension [1]. The simplest case would be to assume that the temperature in the solid is uniform and equal to the melting temperature. Even in that case, for example, if ice melts in a pool of stationary water, a further complication arises due to the anomalous thermal expansion of water at about 4 ^{0}C, which causes a phenomenon called convective inversion [2].
If during the phase change there are fluids consisting of more than one chemical species (for example melting of ice into saline water) then natural convection would be due to the simultaneous action of thermal and solutal driving forces. Many binary fluids could have very different molecular diffusivities for heat and species and such natural convection is often called double diffusive convection [3].
Melting of objects with spherical shapes has received much attention because of experimental and theoretical convenience. The study of thermal free convection from an ice sphere melting in a pool of water, [4], showed that for water temperatures approximately above 5.3 ^{0}C the overall Nusselt number and the melting rate increase with water temperature. A boundary layer of melted liquid is formed at the top of the sphere and flows downwards, separating somewhere ahead of the lower stagnation point. Thereafter the shear layers form a downward moving plume. In experiments with a wax sphere melting into hot water, [5], the melting rates increased almost linearly with pool water temperature difference $\Delta\Theta = (\Theta_{ice} - \Theta_{amb})$, while the downward plume became turbulent and the lower part of the sphere was eroded. In [4], for water temperatures below 4 ^{0}C the opposite phenomenon was observed, i.e. the overall Nu and melting rates decreased as the water temperature increased from 0 ^{0}C to 4 ^{0}C, while the boundary layer initiated at the lower part of the sphere and separated near the top. For water temperatures between 4 ^{0}C and 5.3 ^{0}C the direction of flow is not unique and no boundary layer exists. Findings similar to those reported in [4] were

found in [6]. The degree of melting was proportional to the mean heat transfer coefficient and the temperature difference between the water and the ice and inversely proportional to the sphere diameter D_0. Like in [4], the shape of the sphere changed to look like a prolate spheroid with the major axis, a, in the vertical direction. The eroded region at the bottom of the body subtended an angle from the center of about 38^0. This phenomenon was attributed to the strong circulation in the wake of the boundary layer flow.

The case of an ice sphere melting in still air ($U_{MEAN} = 0$) has not been treated extensively, because most of the work deals with melting in a moving air stream under conditions of forced and mixed convection [7], [8], [9], and also in a moving water stream [10], [11], the last one addressing the effects of strong anisotropic turbulence. In general, the rate of heat transfer between the ice sphere and air of constant temperature and humidity is formulated in [8] as the latent heat of melting to be equal to the heat transfer through water, which in turn would be equal to the sum of the heat conduction and convection through air and the vapour condensation very near to the surface of the sphere. For still air ($U_{MEAN} = 0$), exchange of heat takes place only through conduction and the exchange of water vapour between the sphere and the air is suppressed. Denoting by t_m the time for complete melt since the initiation of melting process, they found that for constant air humidity, D_0^2/t_m varies almost linearly with $\Delta\Theta = \Theta_{amb} - \Theta_{0\ ice}$, the difference in temperature between the ambient air temperature and the initial (t = 0) ice surface temperature. According to [8], in an air stream with $U_{MEAN} \neq 0$, the enhanced exchange of heat and water vapour can be taken into account in the heat transfer coefficient via two numerical constants C_h and C_m as : $C_h \approx 1+ 0.27Re^{1/2}$, $C_m \approx 1 +0.26Re^{1/2}$ where $Re = U_{MEAN}D_0/\nu$ is the Reynolds number of the sphere. Then for constant air humidity, $D_0^2/ (t_m C_m^{0.82})$ increases almost linearly with $\Delta\Theta$.

A study of horizontal water flow around a melting ice sphere with the aid of PIV, [10], showed that the increased circulation in the wake enhances forced convection heat transfer and as a result the shape at the rear becomes flat. Because the separation of the boundary layer and the locally decreased heat transfer there occurs at the position where the maximum diameter of the melting particle aligns in the transverse direction of the mainstream flow, the melting particle is shorter in the direction of the flow and the ratio m of the streamwise to transverse maximum dimensions (m = major axis a / minor axis b, if the shape is a spheroid) is greater than 1.0. The circulation in the wake and the rate of increase of m are intensified as the wake speed increases. Since the experiment in [10] was conducted with the water flowing in the horizontal direction, the contribution of free convection at relatively low water speeds (Grashof/Reynolds^2 > 0.682 in [10]), resulted in melting shapes of non-spheroidal shape, but rather non-symmetric, on account of the downward inclination of the plume of melted liquid.

In meteorology, there is interest in the shape of hailstones which usually, for stability reasons, have the shape of an oblate spheroid with the minor axis, b, in the direction of fall (vertical). Such shapes of ice spheroids were tested in a wind tunnel in [7]. It was found that the total melting rate (kg/s) was proportional to $Re^{1/2}$ and a numerical factor χ (with values between 0.7 and 1.0 in their experiments) which was an increasing function of m, that is, the more "flat" the hailstone, the better the total rate of heat transfer per unit area of surface and the higher the melting rate. The "flatter" hailstone however has relatively smaller total surface area (assuming that the major axis length, a, is the same) and less total mass lost due to melting.

A systematic effect of background turbulence on melting appears only in recent work [11], to the authors' knowledge. The melting of an ice sphere was studied in a turbulence chamber containing two rotating disks which produced strong anisotropic turbulence with nearly zero mean velocity and milder isotropic turbulence with strong non-zero mean velocity, all at high Re numbers. In different versions of the tests, the spheres were kept fixed or allowed to be freely advected in the turbulence chamber. In both cases, as melting progressed, the initial spherical shape changed into that of an ellipsoidal prolate spheroid with the major axis, a, aligning with the direction of the weakest turbulent intensity. Before being inserted into the turbulence chamber the ice spheres were thermalized at their melting temperature of 0 ^{0}C. In one such experiment of anisotropic turbulence with $U_{MEAN} = 0$, $u_{RMS} \approx 0.09$ m/s and the other two turbulence intensities being approximately equal to 0.14 m/s, the initial diameter of the ice ball was $D_0 = 18$ mm. The forced convection was overwhelming natural convection and the convective heat flux was proportional to the temperature difference between the ambient water temperature and the ice temperature, $\Delta\Theta = \Theta_{amb} - \Theta_{ice}$. Since the temperature gradient inside the sphere disappeared due to thermalization, the diffusion term in Stefan's equation, [11] was zero and the melting rate of the particle was expected to be proportional to $\Delta\Theta$. Thus, in [11], they reduced the melting rate to the derivative of the radius of the sphere, dR/dt. Although the heat transfer was observed to be much stronger ($Nu \approx Re^{0.8}$), than in laminar flows, the examined two cases for fixed spheres i.e. $U_{MEAN} = 0$ with 50% anisotropy and $U_{MEAN} \neq 0$ with "nearly" isotropic turbulent flow, led

to similar values of the Nusselt number (directly related to dR/dt). The explanation could be that these two different types of flows had similar large scale Reynolds numbers ($\approx 10^4 - 10^5$). Finally, in the case of freely advected particles with $U_{MEAN} = 0$ and with diameters of the order of the integral scale of turbulence, it was found, [11], that contrary to the fixed particle cases for which the shape of the particle reflected the anisotropy of the flow, the melting was isotropic and going on for hundreds of large eddy turn over time scales ($0.13 \leq T_E \leq 0.675$, observed times in the experiments > 40 s, with dR/dt almost constant in that time period). This fact was attributed to the coupling of the translational dynamics of the freely advected spheres to their rotational dynamics. The Nusselt number was found to be a linear function of the particle Reynolds number, $Nu \approx R$. According to [11], this type of flow round the moving and melting sphere corresponds to the ultimate regime of heat transfer for which the heat transfer coefficient no longer depends on the particle diameter, but it is only proportional to the RMS velocity fluctuations, u_{RMS}.
The purpose of the present experimental work, employing mainly flow visualization, is to investigate the influence of "nearly" isotropic and homogeneous turbulent flow on the melting process of fixed spherical ice balls in both water and air environments. In order to separate the effects of mean flow and isotropy (not pursued in [11]) we concentrate on nearly isotropic turbulent flows with zero mean speed, $U_{MEAN} = 0$. The turbulent flows in water were generated with double oscillating grids [12] and in air with synthetic jets [13]. The main parameter of concern is the changing level of u_{RMS} and its influence on the melting rate. In addition, it is intended to look into the influence of turbulent temperature fluctuations θ_{RMS} on melting, using the synthetic heated air jet facility, a topic not document in the literature.

2 Experimental Setup and Flow Procedures

2.1 The Oscillating Grids in the Water Tank

The experiments with melting ice spheres in water were conducted in a perspex water tank 4 m long (streamwise horizontal, x direction), 0.70 m deep (vertical, z direction) and 0.4 m wide (spanwise, y, direction). At the central region of the tank two vertical biplanar grids oscillating in phase in the x direction produced a nearly isotropic and homogeneous turbulent flow, [12], [13], Fig. 1. The square biplanar oscillating grids were constructed out of hollow 10 mm square aluminum bars forming a mesh size M=62 mm. They were mounted vertically on an overhead frame and spanned the water tank walls, leaving 1 mm gap on either side. The horizontal spacing of the grids was Δx=0.45 m. They were put into a nearly sinusoidal motion by means of an eccentric mechanism run by an electric motor of variable speed, which was therefore linearly related to the oscillation frequency f (Hz). It has been established, [12], [13], that the turbulent velocity fluctuations in the central region between the grids vary linearly with f and $S^{3/2}$, where S is the oscillation half stroke. The results presented in this paper refer to S = 60 mm, i.e $S/M \approx 1$ and $0.56 < f < 2.98$ Hz. Values of u_{RMS} at the center (x = y = z = 0) measured with an LDA, are plotted versus f in Fig. 2. The RMS values of the other two transverse components did not depart by more than 10% from the streamwise component and the mean velocity was an order of magnitude smaller than u_{RMS}. The integral length scale of turbulence was of the order of magnitude of the melting sphere diameter D_0 (= 0.0375m). The region of homogeneity extended over distances ± 0.07 from the center, hence it may be assumed that over this volume the turbulence is nearly isotropic and homogeneous with mean speed $U_{MEAN} \approx 0$. Melting experiments were carried out for u_{RMS} = 0.034, 0.040, 0.044, 0.049, 0.053 and 0.058 m/s. The ambient water temperature in the experiments was $\Theta_{amb} = 15\ ^0C$.

2.2 The Synthetic Air Jets in the Turbulence Chamber

A cubic metal frame frame was constructed with dimensions 1.80 x 1.80 x 1.80 m which formed the basis of an open type "turbulence chamber" facilitating the least optical obstruction to the measurements and flow visualization procedures, Fig. 3. The objective was to produce, as in the oscillating grids facility, a sizable region of nearly homogeneous and isotropic turbulence, with as much as possible low mean velocity, $U_{MEAN} \approx 0$. The four vertical support pylons were 60 mm diameter metal tubes along which articulated blocks, supplied with universal joints and adjustable threaded rod, could slide up and down. At the end of the threaded rods eight 200 mm diameter, 8 Ω, 30 Hz - 5 kHz range loudspeakers were mounted, all pointing towards the center of the cubic arrangement. This rig allowed alteration of the size of the turbulence chamber (larger than reported in the literature so far) and also the alignment of the axes of the loudspeakers (ideally

coinciding with the diagonals of the cube).

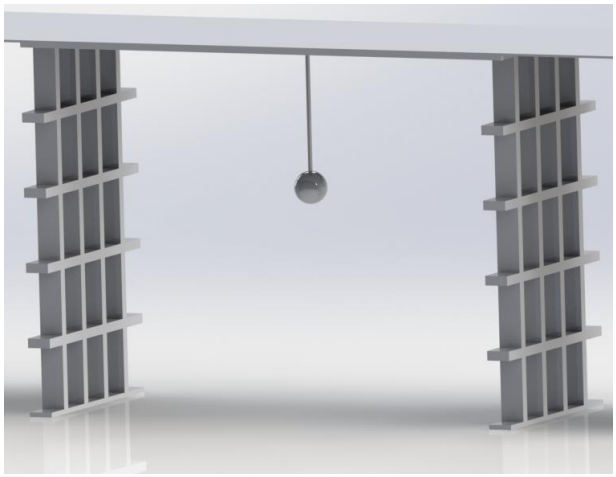

Fig. 1 Oscillating grids and melting sphere at center

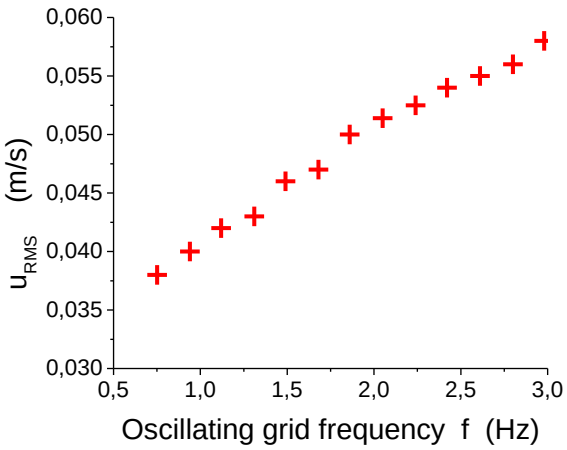

Fig. 2 Turbulence intensity at center

The lack of solid walls, as found in [14], permits better flow visualization and also makes the random phasing in the power supply of the loudspeakers unnecessary, because standing waves and acoustic resonances are minimized. The loudspeakers were driven by power amplifiers up to a maximum 6.25 W / loudspeaker (i.e. total $Power_{max}$ = 50 W) to which sinusoidal signals were fed with frequencies, f, ranging from 40 to 140 Hz. In the present experiments, an alternative method to increase the mass flow rate was introduced i.e. the loudspeakers were capped with common type plastic domestic funnels, 200 mm in diameter and ending to a nozzle of internal diameter D_{NOZZLE} = 14 mm. All nozzles had to be directed exactly towards the center, because misalignment was found to result in U_{MEAN} considerably different from zero [15]. Preliminary tests indeed showed that the turbulence in the center regions was greatly increased and the synthetic jet exit speeds were also very high compared to those of the uncapped loudspeakers. The funnels act as air mass "collectors" and during the outward motion of the loudspeaker membrane, a column of air is ejected towards the cube center. The vortex rings originating at the funnel lips travel fast downstream and break down into turbulence before the suction phase begins, when the membrane retracts backwards. This implied a quite small mass flux across the actuator (however, eventually a function of frequency f), but a net momentum flux imparted to the external flow. The experiments for the present work were conducted with cube side dimension equal to 0.635 m (maximum funnel tip distance along the diagonal direction r was equal to 1.1 m). The air inside the cavity formed by the loudspeaker and the funnel was electrically heated by resistances each of 60W, in order to generate temperature fluctuations θ(t) at the turbulence chamber central area. Velocities were measured with LDA and temperatures with thermocouples and hot wire anemometers set at the Constant Current mode. It was found, [15], that isotropy and homogeneity both in the velocity and temperature fluctuations prevailed over a spherical space of radius from the center of about 0.08m. In the worst cases, U_{MEAN} was less than 15% of the corresponding u_{RMS} and anisotropy less than 10%. The dependence of u_{RMS} at the turbulence chamber center on driving frequency f is shown in Fig. 4. Due to the electromechanical response of the loudspeakers, the cone oscillation decreases as the driving frequency increases and as a result the amount of the expelled air and imparted momentum in each cycle diminishes. This is why u_{RMS} decreases as f increases. Tests for the effect of turbulence on ice melting were performed with turbulence levels of 0.79, 0.64 and 0.47 m/s. The ambient air temperature in the not heated turbulence experiments was Θ_{amb} = 23 ^{0}C.

When heat was applied to the air jets, an "isotropic" (referring to u_{RMS}) thermal turbulence was generated in the central region. The evolution of the mean temperature difference along the funnel centerline direction r, Θ_{CL} - Θ_{amb} , (Θ_{amb} being the ambient air temperature) up to the center of the chamber is shown in Fig. 5 for three turbulence intensities, 0.79, 0.64 and 0.47 m/s. The ambient air temperature in the heated turbulence experiments was Θ_{amb} = 23 ^{0}C. In the central region the mean temperature profile is flat, with higher temperatures associated with lower u_{RMS} and higher frequencies. The same is observed at the funnel exit, because of the reduced flow rate in and out of the cavity at higher frequencies mentioned above. Heat transfer from the heating elements was therefore reduced and there was a net temperature rise.

Fig. 3 Turbulence chamber with synthetic jets.

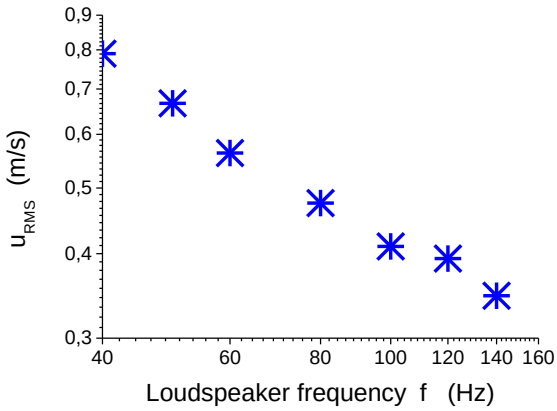

Fig. 4 Velocity fluctuations at the center of the chamber

At about 15 diameters from exit, the individual heated jet flows start to interact with each other and prevent further temperature decay. Fig. 6 shows the effect of turbulence on the levels of mean and fluctuating temperature at the center. Lower values of u_{RMS} lead to higher mean temperatures Θ_{MEAN} and lower temperature fluctuations θ_{RMS}. The effect on Θ_{MEAN} could be attributed to the increased mean temperature at the nozzle, as mentioned before. For the latter, i.e. the increased levels of θ_{RMS} even though the mean temperature is lower, one has to take account the local turbulence structure there, that is the intensity of the velocity fluctuations u(t) and the local scale L_u at which they occur [16]. Intuitively, lower driving frequencies of the loudspeakers would imply longer wavelengths of the columns of air at the nozzle and larger turbulence length scales L_u at the turbulence chamber. This would cause thermal mixing on a larger scale and causing bigger differences between warm air and ambient air and bigger θ_{RMS} as compared to the higher driving frequencies and shorter wavelengths. Although no quantitative results are available yet, preliminary observations with smoke flow visualization and shape of the θ(t) signal, are in support of this conjecture.

2.3 Models and Flow Visualization

The ice spheres were made using table tennis plastic balls which were filled with water and allowed to freeze at -15 ^{0}C with a supporting Teflon threaded rod 5 mm in diameter inserted into the mould. The plastic cover was removed before carrying out the experiments in water or air and the sphere was positioned at the center of the facility (water tank or turbulence chamber). For the experiments in water the single sphere had the support rod mounted on the upper side (melted liquid flowing downwards away from the rod) while in air, the support rod was mounted on the lower side (melted liquid flowing downwards towards the rod). This would have some repercussions on the local heat transfer and on the changing shape of the melting ball, as will be discussed later. In some spheres a thin thermocouple was embedded in the center of the sphere in order to monitor the change of its core temperature, Θ_{CORE} , with time t and get an idea about the diffusion of heat into the sphere during melting. The ice spheres were not thermalized to 0 ^{0}C, as in [11] and as a result the melting occurred simultaneously with a gradual rise of the core temperature, as shown in Fig. 7, the experiment being performed in the water tank for two turbulent intensities u_{RMS} = 0.044 and 0.053 m/s. It appears that stronger turbulence causes heat from the surrounding water of temperature Θ_{amb} = 15 ^{0}C to penetrate faster the interior of the ice sphere, keep the sphere "thermalized" at 0 ^{0}C over a shorter period and eventually lead to shorter total melting time t_m.

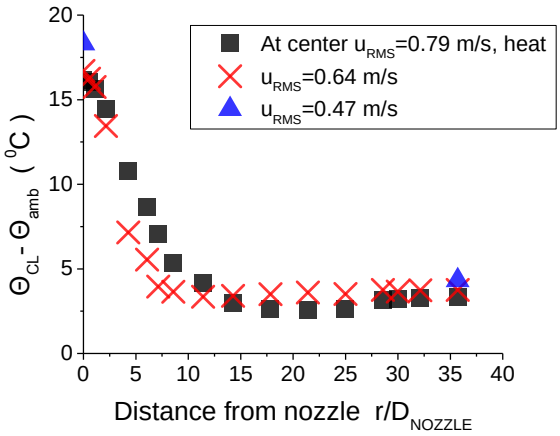

Fig. 5 Mean temperature difference along nozzle centerline

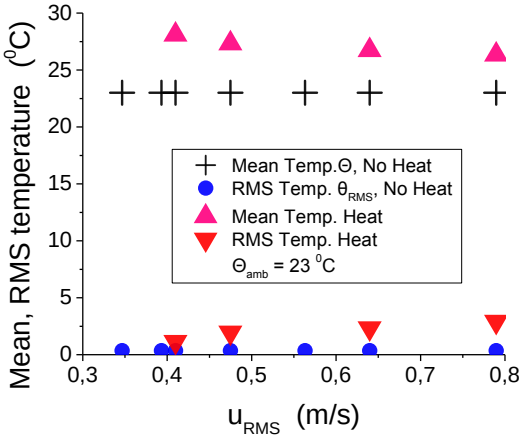

Fig. 6 Mean and RMS temperatures at chamber center

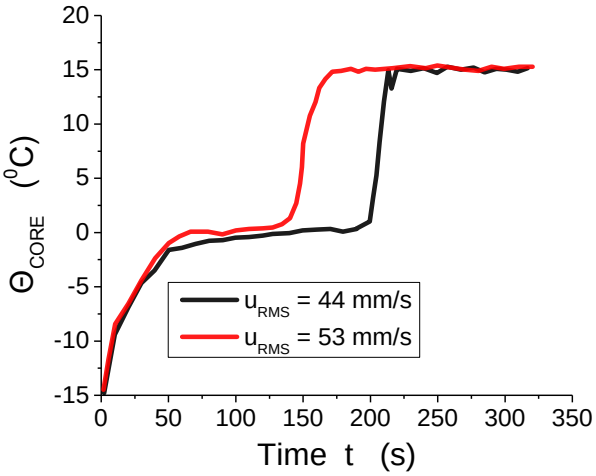

Fig. 7 Evolution of the mean temperature Θ_{CORE} at the center of the melting sphere in water, $\Delta\Theta$=30 ^{0}C

The main quantitative method for the study of the melting phenomena was flow visualization using normal video or still pictures starting from time t = 0 (initiation of melting process) till the occurrence of complete melt at t = t_m. The sphere was observed from front and top views and image processing was employed to yield the variation of its linear dimensions with time, after appropriate scaling. The quantities of length that are presented in the following and which are believed to describe rather accurately the evolution of melting and also be comparable to those reported in the literature, are the hydraulic diameter defined here as $D_H(t)$ = 4 x AREA / PERIMETER and the lengths of the major and minor dimensions during melting, to be associated with the major, a, and minor, b, axes of spheroids found in the literature. AREA is the projected area of the sphere calculated from the image processing software (usually in mm^2) and PERIMETER is the melting contour perimeter calculated likewise (usually in mm).

A qualitative study of the whereabouts of the melted liquid in the water tank tests was carried out by using Laser Induced Fluorescence (LIF). The ice balls were made out of a mixture of water with a small quantity of Rhodamine G (≈ 30 ppm) and the flow was illuminated by a laser light sheet. An Argon ion laser at 514 nm wavelength was employed for that purpose aligned with a 9 side rotating polygonal mirror prism in order to produce the vertical light sheet in the horizontal or vertical directions. Short video recordings were made in these tests of duration 3 s but at a rate of 240 frame/s.

3 Results and Discussion for Melting in Water

3.1 Measurements of Diameters and Melting Times for a Single Sphere

The variation of the hydraulic diameter $D_H(t)$ of the ice sphere with time t, for various levels of turbulence intensity u_{RMS} and also in still water is shown in Fig. 8 for temperature difference $\Delta\Theta = \Delta\Theta = 30\ ^0$C.

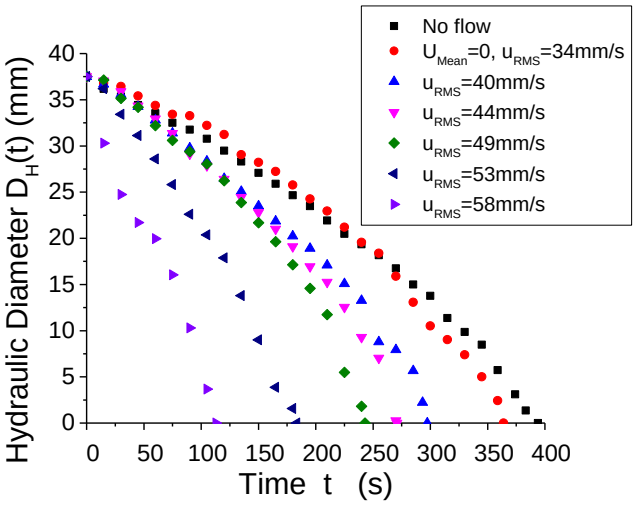

Fig. 8 Hydraulic diameter of melting ice spheres in water for various levels of turbulence, $\Delta\Theta$=30 ^{0}C

It is observed that the stronger the turbulence the higher is the heat transfer to the sphere and the faster the melting rate. The slow motion of the grids and their resulting weak turbulence tend to affect melting only at a later stage, owing also to the slow penetration of heat into the sphere as discussed earlier. The remarkable impact of strong turbulence on the melting process should be related to changes in the behavior of the boundary layers and the local heat transfer around circumference as noticed also in non melting bodies, but also to the fact that strong turbulence is able to transport away cold melted fluid and overcome buoyancy forces that may locally inhibit melting. From Fig. 8, the complete melting times, t_m , were computed (when $D_H(t) \approx 0$) and the results are plotted against u_{RMS} in Fig. 9.

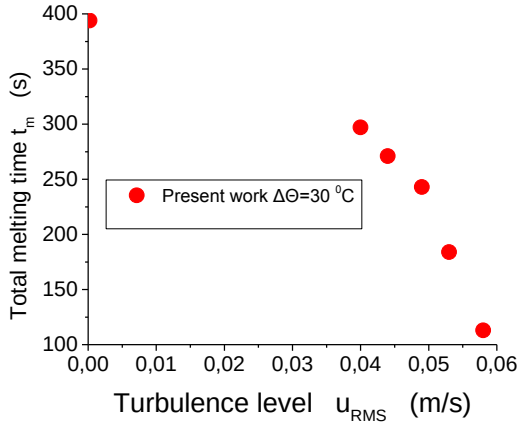

Fig. 9 Melting times t_m of ice spheres in water for various levels of turbulence, $\Delta\Theta$=30 ^{0}C

It is found that the melting time in the strongest turbulence case of u_{RMS} = 0.058 m/s is almost one fourth of the corresponding time for melting in still water of the same temperature difference $\Delta\Theta = 30\ ^0$ C. The parabolic form of the plot indicated that turbulence has a stronger than linear influence on the melting time. The fact that the melting rate changes appreciably, depending on the flow conditions and the time t itself can

be visualized if a dimensionless melting rate L is introduced such that $L = (-dD_H(t) / dt) / (D_0 / t_m)$, that is the instantaneous melting rate is normalized with an average melting rate D_0 / t_m . Fig. 10 shows the evolution of L with time t for various types of flow. There is also comparison with some experimental data from other workers, which however do no exactly match the present experimental conditions.

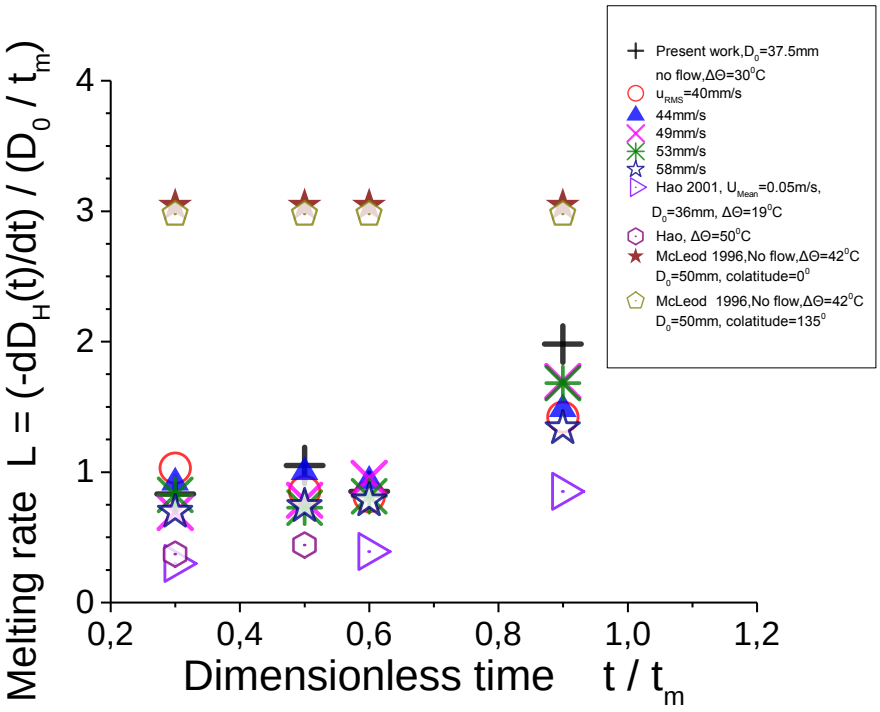

Fig. 10 Dimensionless melting rates under free and forced convection

The non dimensionalizing parameter is very small for melting in still water because t_m is always big, therefore L is small for high melting rates as it happens when turbulence is present. L also tends to increase with increasing time, reflecting the drop rate in $D_H(t)$ shown in Fig. 8. The present data for L are close to those reported in [10] with similar $\Delta\Theta$ and D_0 which however refer to melting in a horizontal water stream (U_{MEAN} = 0.05 m/s) without turbulence. It seems as if forced convection without turbulence brings about similar changes in the sphere size as turbulence without a mean velocity, as in the present experiments. The results of [5], appearing also in Fig. 10, come from experiments of melting spheres made out of polyethylene glycol 600 (PEG 600 , soluble in water) in still hot water. The melting liquid formed a thin layer on the sphere surface and being heavier than the water, it sank to form a turbulent plume at a distance of the order of the sphere diameter. This phenomenon induced different rates of melt on the sphere surface and in Fig. 10 the rates of melt at colatitude angles φ (from the top) 0^0 and 135^0 are shown. In [5], L(t) remains constant with time because it was found that the radius of the sphere at various angles φ decreased linearly with time and the melting rate changed linearly with temperature difference.
A general finding from previous work, e.g. [5], [11], both for $U_{MEAN} = 0$, is that the total heat flux and consequently the melting rate increases linearly with $\Delta\Theta$. In [6] the degree of melting was normalized with $\Delta\Theta$ and D_0 , the initial diameter of the sphere, thus forming a normalized Nusselt number $Nu_N \sim (-D_0^2\, dD_H / dt) / \Delta\Theta$. Nu_N is plotted against u_{RMS} in Fig. 11. Our results agree with those in [6] which refer to still water (no flow, $U_{MEAN} = 0$). The present experimental data indeed show that Nu_N and heat transfer rate increase with turbulence intensity, as also reported in [11]. The two experimental points in Fig. 11, connected with a straight line, one from the present work and the other from [11] were found to have similar Nusselt numbers computed from the relationship between the Nusselt number and the Reynolds number and based on the u_{RMS} as the characteristic velocity. It may again be argued that turbulence without a mean velocity could cause effects that would bring a rise in the Reynolds number with finite mean velocity, in other words, turbulence acts as an effective increase in the Reynolds number.

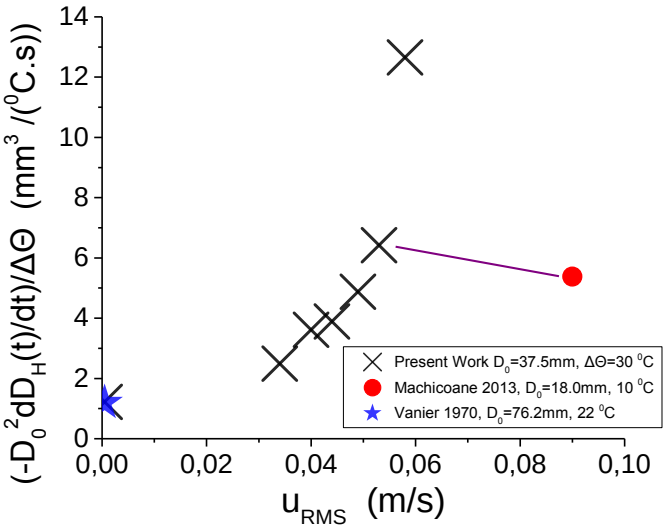

Fig. 11 Degree of melting normalized with temperature difference ΔΘ and initial diameter D_0

Fig. 12 shows the deviation from the spherical shape, as melting progresses. A measure of this deviation is the ratio of the major to the minor axis length m(t) = a(t) / b(t) at every time t. Our results indicate that the stronger the turbulence, the higher m becomes, i.e. deformation is enhanced. It is expected that m would be affected by the manner it is positioned with respect to the direction of the flow (horizontal flow or vertical flow would give different results). Also, the way it is mounted in the experiments with still water would play a role. Some workers used wires to suspend the sphere, which was the best because of least heat transfer loss to the supports. In our experiments the sphere was held facing the water downwards from the metal plate above the tank by means of a rather thick plastic rod (see section 2.3). Due to the oscillating grids wires or thinner rod could not be used due to excessive vibration. Although the heat transfer to the plastic may not be severe, it is recognized that the existence of a plastic insert should bring some asymmetry in the shape of the sphere as it melts. Comparison with experimental data from other workers reveals the same trend, the factor m increases with time a, but which direction in enhanced is related to the characteristics of the ambient medium with respect to the buoyancy forces [5], [6] when $U_{MEAN} = 0$, the orientation of mounting with respect to the main flow, [10], the method of mounting the supports (present work, [6]) and the direction of the weakest turbulence intensity ([11], see also section 1).

3.2 Changing Diameters and Melting Times for a Pair of Spheres

A first result on the role of proximity of two spheres on their melting with turbulence level $u_{RMS} = 0.053$ m/s is given in Fig. 13. In one occasion two ice spheres were held with their vertical axes in the same vertical line and at spacing $2D_0$ apart. In the other, the upper sphere was ice and the lower sphere was plastic (no melting). The instantaneous hydraulic diameter, non dimensionalized by the initial diameter is plotted against time. In the first case, this ratio concerns the lower sphere, in the second case the upper sphere. The single sphere result is also included for comparison. It can be seen that in the first case the lower sphere melting is delayed after some time because of the cold plume from the upper melting sphere which flows downward, despite the agitation of turbulence. Initially the melting process of both ice spheres is not altered significantly, being similar to the single sphere melting process. At a time by which the isolated sphere would have been "thermalized" to 0 ^{0}C (see Fig. 7), the melting modes of the spheres change behavior and the lower sphere appears to be influenced by the plume of the upper sphere. The ratio $D_H(t)/D_0$ at this time is about 0.67. The time for complete melting tends to be extended. In the second case, the upper sphere melting behavior is affected by the presence of the lower plastic sphere relatively later, when $D_H(t)/D_0$ is about 0.4 probably due to local changes in the turbulence field, which may be more important for a sphere of smaller size ($D_H(t) \approx 0.4\ D_0$). Further results will be presented in a future work.

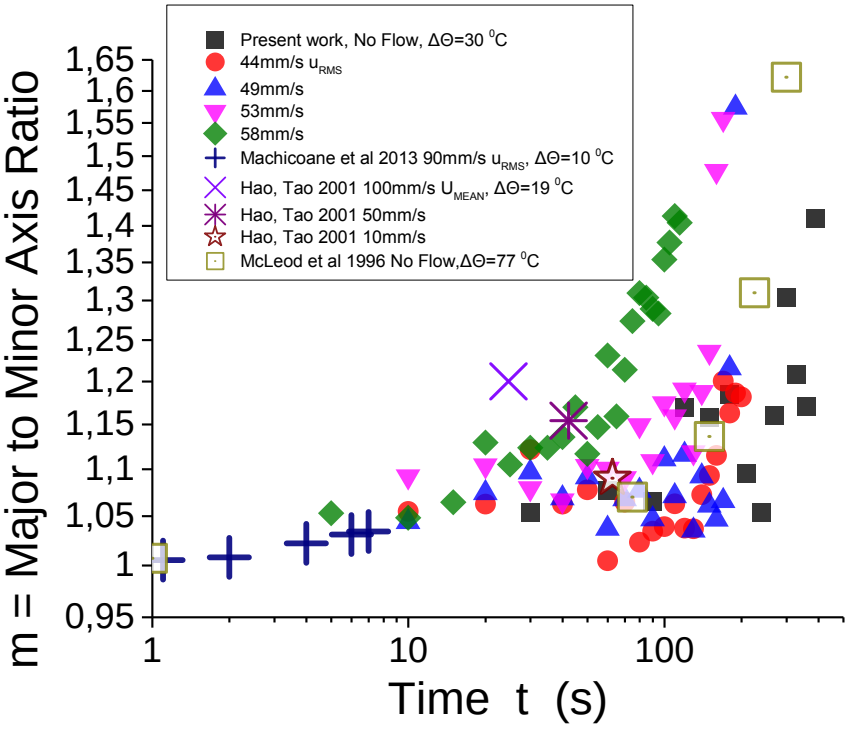

Fig. 12 Deviation from the initial spherical shape during melting

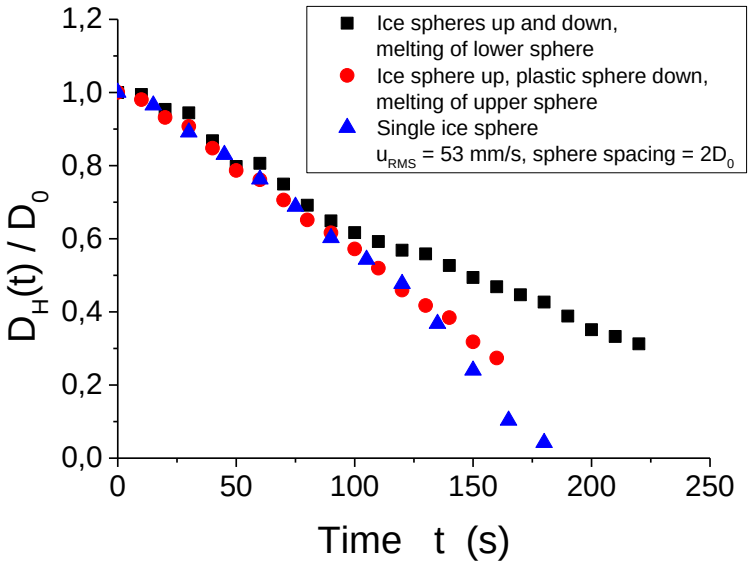

Fig. 13 Effect of proximity of two spheres on melting

3.3 Flow Visualization with LIF

Figures 14a, 14b and 14c show some of the results of flow visualization with LIF and increasing unsteadiness in the flow, i.e. still water, very weak motion of the grids and stronger motion of the grids (imposing turbulent flow). The melted water moves steadily downwards when there is no flow. In the weak turbulence the cold negatively buoyant plume begins its unsteady motion and in the strong turbulence it moves in different directions and mixes effectively with the surrounding fluid.

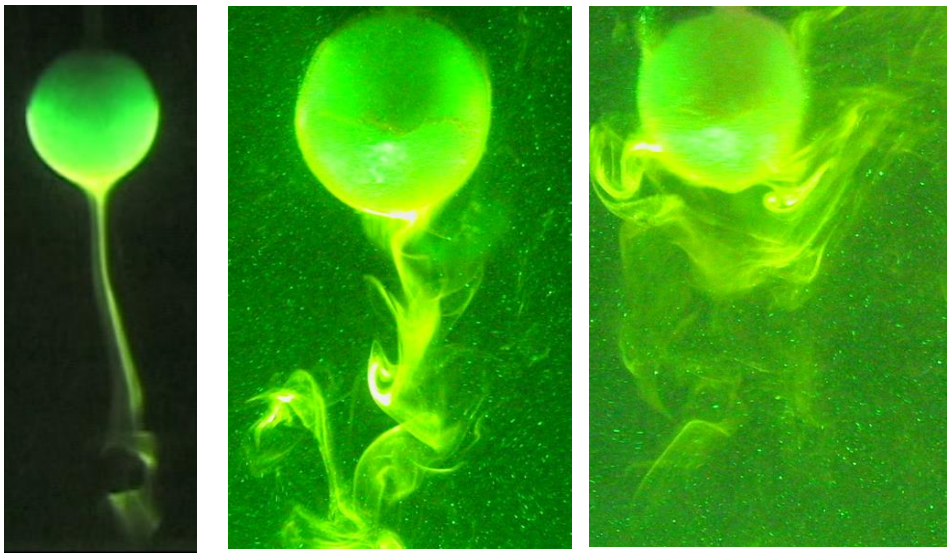

a **b** **c**

Figs. 14a, b, c Flow visualization with LIF for still water, very weak flow unsteadiness and stronger turbulence

4 Results and Discussion for Melting in the Turbulence Chamber

The decrease with time of the hydraulic diameters of the melting ice spheres in the synthetic jet turbulence chamber is shown in Fig. 15 for heated and unheated turbulent flow. In both cases the ambient air temperature was 23 ^{0}C and the initial ice sphere temperature -15 ^{0}C. As found in the experiments with turbulence in water, here also there is a decay of $D_H(t)$ with time in the unheated and heated cases. Although the turbulence intensities are an order of magnitude larger than those in water, the melting times are here one magnitude bigger, reflecting the reduced heat transfer coefficients in air. Melting in still air needs again considerably more time compared to melting under turbulent flow conditions. The contribution of temperature fluctuations, θ_{RMS} , on the decay of the sphere size, for the same value of turbulent velocity fluctuations is evident in Fig. 15 at the highest value examined, u_{RMS} = 0.79 m/s. From Fig. 6, for the unheated turbulence case Θ_{MEAN} = 23 ^{0}C, θ_{RMS} = 0.35 ^{0}C, while for the heated case Θ_{MEAN} = 26.35 ^{0}C, θ_{RMS} = 2.89 ^{0}C. The initial impact of heat on the reduction of $D_H(t)$ is strong, up to the time where the size of the sphere has been reduced by about 50%, after which time the role of heated turbulence seems to be not so important. A question remains about which factor plays more important role in the decay of $D_H(t)$, the increased mean temperature or the increased temperature fluctuation. For the weaker turbulence with u_{RMS} = 0.47 m/s, the mean temperature difference in comparison to $\Delta\Theta$ for u_{RMS} = 0.79 m/s is roughly doubled (= 5.82 ^{0}C, while the corresponding θ_{RMS} is roughly halved (= 1.2) ^{0}C. Yet, it performs better on the decay of $D_H(t)$ than the stronger heated turbulence with u_{RMS} = 0.64 m/s, $\Delta\Theta$ = 3.8 ^{0}C, θ_{RMS} = 2.3 ^{0}C. Other factors like air humidity and turbulence length scale may also play a role. In [8], the melting time t_m is related to the mean temperature difference $\Delta\Theta = \Theta_{amb} - \Theta_{ice}$ for different air speeds of constant humidity, with the effect of varying the Re number taken into account, and the results are shown in Fig. 16. Our results for still air and strong heated turbulence are included in the plot. The role of forced convection caused by an air stream is evident as well as the importance of $\Delta\Theta$.

5 Conclusions

The decrease in the size of ice spheres melting in water and air is greatly influenced by the presence of turbulence. More intense are the phenomena in water. Nearly isotropic and homogeneous turbulence with zero mean velocity reduces the melting times significantly in comparison to melting in still fluid. Buoyancy forces, in combination with the effects of turbulence may lead to deformation of the sphere into a spheroid during the melting process. Analogous phenomena have been observed by previous workers when melting occurs by forced convection due to an air or water stream, and in which the mean temperature difference is

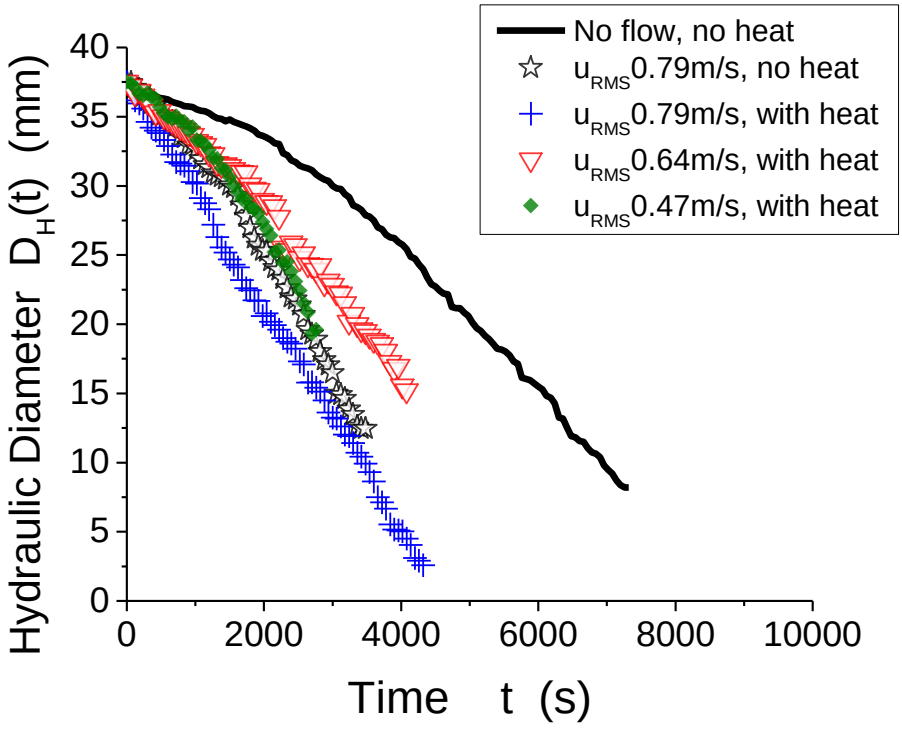

Fig. 15 Variation of the hydraulic diameter of ice spheres in the turbulence chamber with heated and unheated air

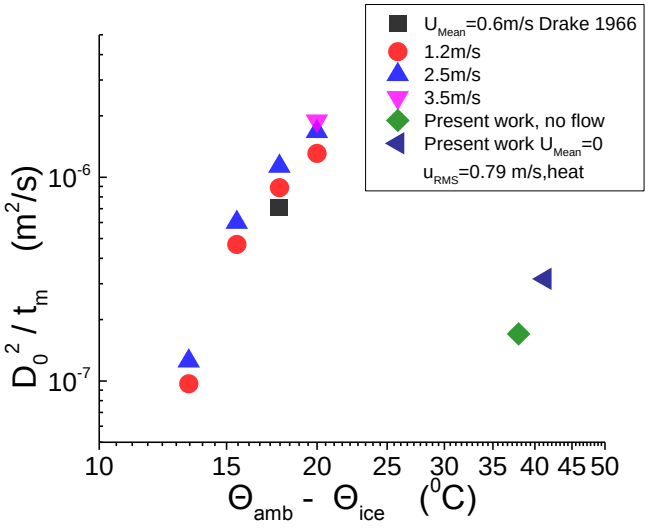

Fig. 16 Dependence of melting time on ΔΘ for melting spheres in an air stream.

proportional to the decay rate of the linear dimensions, like the sphere diameter. Due to some analogy in the behavior of melting rates with turbulence but with zero mean velocity and the melting rates without turbulence but with finite mean velocity, it is conjectured that turbulence acts as an effective increase in the Reynolds number. When turbulent velocity fluctuations are accompanied by turbulent temperature fluctuations the melting rates are further enhanced. The melting of a pair of spheres showed the importance of buoyancy forces owing to the dispersed cold melting fluid affecting the melting of the spheres.

References

[1] Hu H., Argyropoulos S.A. (1996). Mathematical modelling of solidification and melting: a review. *Modelling Simul. Mater. Sci. Eng.,* vol. 4, pp 371-396
[2] Merck H. J. (1954). The influence of melting and anomalous expansion on thermal convection in laminar boundary layers. App. Sci. Res., vol. 4, pp 435-452
[3] Beckermann C., Viskanta R. (1988). Double-diffusive convection due to melting. *Int. J. Heat Mass Transfer*, vol. 31, pp 2077-2089
[4] Schenk J., Schenkels F.A.M. (1968). Thermal free convection from an ice sphere in water. *Appl. Sci. Res*., vol. 19, pp 415-476
[5] McLeod D.S., Riley D.S., Sparks R.J. (1996). Melting of a sphere in hot liquid. *J. Fluid Mech*., vol. 327, pp 393-409
[6] Vanier C.R., Tien C. (1970). Free convection melting of ice spheres. *AIchE Journ*., vol. 16, pp 76-82
[7] Macklin W.C. (1963). Heat transfer from hailstones. *Quart. J. Roy. Met. Soc*., vol. 89, pp 360-369
[8] Drake J.C., Mason B.J. (1966). The melting of small ice spheres and cones. *Quart. J. Roy. Met. Soc*., vol. 92, pp 500-509
[9] Goyer G.G. Lin S.S., Gitlin S.N., Plooster M.N. (1969). On the heat transfer to ice spheres and the freezing of spongy hail. *Journ. Atm. Sci*., vol. 26, pp 319-326
[10] Hao Y.L., Tao Y.X. (2001). Melting of a solid sphere under forced and mixed convection: Flow characteristics. *ASME Journ. Heat Transfer*, vol. 123, pp 937-950
[11] Machicoane N., Bonaventure J., Volk R. (2013). Melting dynamics of large ice balls in a turbulent swirling flow. *Physics of Fluids*, vol. 25, pp 1251011-12510110
[12] Stapountzis H., Zisimatou A., Papanicolaou P. (2010). Study of a dense contaminant dispersion in rectangular cavities using LIF. ISFV14 - 14th International Symposium on Flow Visualization EXCO Daegu, Korea
[13] Srdik A., Fernando H.J.S., Montenegro L. (1996). Generation of nearly isotropic turbulence using two oscillating grids. *Experiments in Fluids*, vol. 20, pp 395-397
[14] Hwang, W., Eaton, J.K. (2004). Creating homogeneous and isotropic turbulence without a mean flow. *Experiments in Fluids*, vol. 36, pp 444-454
[15] Stapountzis H., Charalampous G., Tziourtzioumis D., Stamatelos A. (2013). Diffusion in synthetic jet generated turbulence. 4th International Conference on Jets, Wakes and Separated Flows, ICJWSF2013, Nagoya, Japan
[16] Stapountzis H., Sawford B.L., Hunt J.C.R. (1986). Structure of the temperature field downwind of a line source in grid turbulence. *J. Fluid Mech*., vol. 165, pp 401-424